



# Oriented Au nanoplatelets on graphene promote Suzuki-Miyaura coupling with higher efficiency and different reactivity pattern than supported palladium



Natalia Candu<sup>a</sup>, Amarajothi Dhakshinamoorthy<sup>b</sup>, Nicoleta Apostol<sup>c</sup>, Cristian Teodorescu<sup>c</sup>, Avelino Corma<sup>d</sup>, Hermenegildo Garcia<sup>d,\*</sup>, Vasile I. Parvulescu<sup>a</sup>

<sup>a</sup> Department of Organic Chemistry, Biochemistry and Catalysis, University of Bucharest, Bulevardul Regina Elisabeta nr. 4-12, 030018 Bucharest, Romania

<sup>b</sup> School of Chemistry, Madurai Kamaraj University, Madurai 625 021, Tamil Nadu, India

<sup>c</sup> National Institute of Materials Physics, Atomistilor 105b, 077125 Magurele-Ilfov, Romania

<sup>d</sup> Instituto de Tecnología Química CSIC-UPV, Universitat Politècnica de Valencia, Av. de los Naranjos s/n, 46022 Valencia, Spain

## ARTICLE INFO

### Article history:

Received 8 March 2017

Revised 27 April 2017

Accepted 28 April 2017

### Keywords:

Heterogeneous catalysis

Facet 111 oriented Au nanoplatelets

Graphene supported Pd/G and Pt/G

Suzuki-Miyaura couplings

Poisoning effect of halides

## ABSTRACT

Facet 111 oriented Au nanoplatelets (20–40 nm wide, 3–4 nm height) grafted on graphene ( $\overline{Au}/fl-G$ ) are about three orders of magnitude more efficient than Pd nanoparticles supported on graphene to promote Suzuki-Miyaura coupling. In contrast to Pd catalysis, it is shown here that the product yields in Suzuki-Miyaura coupling catalyzed by Au nanoparticles follow the order chlorobenzene > bromobenzene > iodobenzene. Kinetic studies show that this reactivity order is the result of the poisoning effect of halides for Au that is much higher for  $I^-$  than  $Br^-$  and much higher than for  $Cl^-$ , due to adsorption. This strong iodide adsorption leading to Au catalyst deactivation was predicted by DFT calculations of Au clusters.  $\overline{Au}/fl-G$  are about one order of magnitude more efficient than small Au nanoparticles (4–6 nm) obtained by the polyol method supported on graphene. Our results can have impact in organic synthesis, showing the advantage of  $\overline{Au}/fl-G$  as catalyst for Suzuki-Miyaura couplings.

© 2017 Elsevier Inc. All rights reserved.

## 1. Introduction

Cross coupling reactions are among the most versatile transformations in modern organic synthesis due to the high yields that can be achieved, their compatibility with a large number of functional groups and the mild conditions required [1–3]. Among the various cross coupling reactions [4], the Suzuki-Miyaura reaction of phenylboronic acid and aryl halides is the one that has probably attracted the largest attention, due to the difficulty to form C–C bonds among  $sp^2$  carbon atoms and also because this reaction gives access to important chemicals used as therapeutical drugs [5–7], pesticides and as specialty chemicals [8].

Most of the cross coupling reactions, including the Suzuki-Miyaura coupling, are catalyzed by Pd, either as metal complexes or as nanoparticles (NPs) [9–11]. Pd-complexes of substituted biphenylphosphine ligands have been found to be highly active homogeneous catalysts for this process [12,13]. It has been proposed that the reason for this general catalytic activity of Pd arises from its ability to undergo reversible redox cycling and

transmetalation [14]. Particularly the facile swing between Pd(0) and Pd(II) in oxidative additions and the reverse in reductive eliminations is considered crucial for the catalytic activity in coupling reactions when using molecular Pd complexes [14].

In the case of Suzuki-Miyaura coupling catalyzed by Pd, it has been well established that the reactivity order follows the strength of the C–X bond and aryl iodides react much faster than bromides, the coupling occurring in much lower yields for aryl chlorides [15,16].

Besides Pd-complexes, Pd NPs either as colloid or as supported on insoluble solids have also been widely used as catalysts for carbon-carbon bond-forming reactions, such as Suzuki-Miyaura cross-coupling reactions [17–22]. Although supported Pd NPs allow easy catalyst recovery and their reuse, the issues of the lower activity of these heterogeneous Pd catalysts, the occurrence of Pd leaching with high activity of leachate and the general tendency to deactivate are serious drawbacks compared to Pd complexes. Thus, while catalysis by Pd NPs is typically performed under heating or reflux conditions [17,19,23,24] cross-coupling reaction catalyzed by phosphine-stabilized Pd NPs can be carried out at room temperature [25].

\* Corresponding author.

E-mail address: [hgarcia@qim.upv.es](mailto:hgarcia@qim.upv.es) (H. Garcia).

In comparison with Pd, other transition metals are considered much less general and efficient catalysts to promote coupling reactions [26,27]. Specifically in the case of Au, although the number of studies is still very scarce, Suzuki-Miyaura and Sonogashira C–C coupling reactions have been reported [28–33].

The lower catalytic activity of Au NPs does not fit well with the somehow unexpected ability of small Au NPs (<5 nm) to catalyze the coupling of chlorobenzene and phenylboronic acid [28]. Chlorobenzene exhibits low reactivity for cross coupling using Pd catalysts. In the case of Au catalysts, the yield of biphenyl decreases from 87% to 76% and 10% when the size of NPs increases from 1 to 2 and 5 nm and no coupling occurs for samples with Au NP size larger than 10 nm [28]. Chaudhary et al. showed that the support plays a crucial role in the catalytic activity of Au NPs as Suzuki-Miyaura catalysts, basic alkaline earth oxides being the most appropriate ones among a variety of other metal oxides [29]. Thus, using MgO as a support for Au NPs, high biphenyl yield for iodobenzenes and bromobenzenes were reached, but for chlorobenzenes, poor yields were obtained. The catalytic activity of Au NPs-graphene oxide nanocomposite has also been reported for Suzuki-Miyaura coupling reaction of chlorobenzene and phenylboronic acid [30]. Interestingly, the reaction of phenylboronic acid with bromobenzene and chlorobenzene in the presence of Au NPs/graphene oxide nanocomposite was reported to be 95% and 96% yield of biphenyl, respectively, while the use of iodobenzene gave 38% of the yield. Therefore, some unexpected lower activity of iodobenzene observed and attributed to the structure and properties of the support.

Considering the present interest in Au catalysis [34] and the contrasting reports on the reactivity order of aryl halides, it is still pertinent to provide a rationalization of the relative reactivity of aryl halides in Au catalysis and what can be the influence of the preferential crystal morphology, facet orientation and strong grafting on the graphene sheet on the activity of Au NPs.

In the present manuscript the existing data about the activity of supported Au NPs have been complemented by showing that Au grafted on graphene may exhibit three orders of magnitude higher activity than an analogous Pd-graphene catalyst and that Au-graphene presents an opposite reactivity order than Pd-graphene for aryl halides, catalyzing the coupling of chlorobenzene with phenylboronic acid with higher yields than the couplings of bromobenzene and iodobenzene. This reverse product yield of Au vs. Pd has not been reported in the literature so far and it will be shown to derive from the strong poisoning effect of iodide, and in lesser extent by Br, on Au NPs. A rationale for this poisoning effect is proposed based on kinetics study and reported quantum chemical calculations on models of these Au NPs.

Another aspect of our study is to show that 111-facet oriented Au nanoplatelets supported on G exhibit, in spite of their much large particle size, about one order of magnitude higher catalytic activity in the Suzuki-Miyaura coupling than analogous small size Au NPs prepared by the polyol method and supported on G lacking this strong grafting and orientation. In fact, herein we report activity for Au platelets with particle size 20–40 nm that according to the literature should be catalytically inactive [28].

## 2. Experimental section

### 2.1. Catalysts preparation

#### 2.1.1. Synthesis of few-layers graphene (fl-G)

Sodium alginate (Sigma) was pyrolyzed under argon atmosphere heating according to the following program: annealing at 200 °C for 2 h holding time, ramp at 10 °C/min up to 900 °C with 6 h holding time. The resulting carbonaceous residue was

sonicated at 700 W for 1 h in water and the unsuspended particles were removed by centrifugation to obtain fl-G dispersed in water. Water was removed by freeze-drying at room temperature to obtain fl-G as powder.

#### 2.1.2. Au NPs deposition on fl-G (0.1 wt%)

fl-G obtained from pyrolysis of alginate as described above (100 mg) was added to ethylene glycol (40 mL) and the suspension was sonicated at 700 W for 1 h to obtain dispersed fl-G. HAuCl<sub>4</sub> (0.2 mg) was added to the suspension of ethylene glycol containing fl-G and Au metal reduction was then performed at 120 °C for 24 h under vigorous magnetic stirring (500 rpm). The Au/G was recovered by filtration and washed thoroughly with water and with acetone. The Au/G was dried in a vacuum desiccator at 110 °C to remove the remaining water. Analysis of gold present on the powders was determined by ICP-OES (Agilent Technologies, 700 Series) by suspending the powders in aqua regia at room temperature for 3 h and analyzing the Au content of the resulting solution. Pd/G and Pt/G were prepared by following the same procedure using Pd(OAc)<sub>2</sub> (5.5 mg) and Na<sub>2</sub>PtCl<sub>6</sub>·6H<sub>2</sub>O (6.0 mg), respectively.

#### 2.1.3. Synthesis of oriented Au NPs over few-layers graphene films ( $\overline{Au}/fl-G$ )

0.5 g of chitosan from Aldrich (low molecular weight) was dissolved in water by adding acetic acid (0.23 g). Impurities accompanying the commercial sample of chitosan were removed by filtering the solution through 0.45 μm syringe. The viscous solution (500 μL) was cast as nanometric film on quartz plates (2 × 2 cm<sup>2</sup>) spinning at a rate of 4000 rpm during 1 min. Then, the resulting chitosan film was immersed in a HAuCl<sub>4</sub> solution (0.01 mM) during 1 min to adsorb Au. Similar procedure was followed to incorporate Pd<sup>2+</sup> and PtCl<sub>6</sub><sup>2-</sup> using 0.01 mM solutions of PdCl<sub>2</sub> and Na<sub>2</sub>PtCl<sub>6</sub>, respectively. Pyrolysis of the resulting alginate films containing the transition metals was performed under argon atmosphere heating according to the following temperatures and times: ramp 5 °C/min up to 900 °C with a holding time of 2 h. Analysis of metals present on the films was made by immersing the plates at room temperature into aqua regia for 3 h and determining the Au or Pt content of the resulting solution by ICP-OES.

### 2.2. General procedure for the Suzuki coupling of phenylboronic acid with halobenzenes

All reagents were purchased from Sigma-Aldrich and used as received without further purification. To a solution of halobenzene, (2 mmol) in 20 mL of deionized H<sub>2</sub>O was added to phenylboronic acid (2.4 mmol), NaOH (8 mmol) and catalyst. The catalyst was suspended by sonication in the case of Au/G powders or introduced in the reactor as 1 × 1 cm<sup>2</sup> film on quartz in the case of  $\overline{Au}/fl-G$ . The resulting mixture was stirred under reflux at 80 °C for 24 h. The reaction mixture was filtered, then extracted with diethyl ether (3 × 10 mL) and the combined organic layer was dried over Na<sub>2</sub>SO<sub>4</sub>, filtered and concentrated. All samples were derivatized to their trimethylsilyl ethers with BSTFA+TMCS (99:1) before analysis on GC-MS. The products were analyzed and identified using GC-MS (THERMO Electron Corporation instrument).

The analysis of the reaction products was carried out by GC-MS (THERMO Electron Corporation instrument), Trace GC Ultra and DSQ, TraceGOLD: TG-5SilMS column with the following characteristic: 30 m × 0.25 mm × 0.25 μm working with a temperature program (50 °C (2 min) to 250 °C at 10 °C/min (Hold 10 min) for a total run time of 32 min) at a pressure of 0.38 Torr with He as the carrier gas. MS identification of the products: Biphenyl: GC-MS, (*m/z*): 154 (M<sup>+</sup>, 100), 128 (6), 115 (4), 76 (14), 63 (5), 51 (6); o-iodobiphenyl: GC-MS, (*m/z*): 280 (M<sup>+</sup>, 33), 152 (100), 127 (14),

76 (26), 63 (11); *p*-iodobiphenyl: GC-MS, ( $m/z$ ): 280 ( $M^+$ , 23), 152 (100), 127 (30), 76 (40), 63 (15); *o*-bromobiphenyl: GC-MS, ( $m/z$ ): 234 ( $M^+$ , 33), 232 (36), 153 (32), 152 (100), 126 (13), 76 (48), 63 (19); *p*-bromobiphenyl: GC-MS, ( $m/z$ ): 234 ( $M^+$ , 47), 232 (56), 153 (35), 152 (100), 76 (49), 63 (15); *o*-chlorobiphenyl: GC-MS, ( $m/z$ ): 188 ( $M^+$ , 30), 153 (10), 152 (25), 75 (100), 69 (16), 57 (23), 51 (13); *p*-chlorobiphenyl: GC-MS, ( $m/z$ ): 188 ( $M^+$ , 11), 152 (35), 75 (100), 69 (13), 57 (16), 51 (10).

The contents of gold, platinum and palladium in the reaction products were checked by ICP-OES (Agilent Technologies, 700 Series) after calibrating the instrument with standard solutions.

### 2.3. Catalysts characterization

XPS measurements were performed at normal emission in a Specs set up, using Al  $K_{\alpha}$  monochromated radiation ( $h\nu = 1486.7$  eV) of an X-ray gun, operating with 300 W (12 kV/25 mA) power. A flood gun with electron acceleration at 1 eV and electron current of 100  $\mu$ A was used in order to avoid charge effects. Photoelectrons are energy recorded in normal emission using a Phoibos 150 analyzer, operating with pass energy of 30 eV. The XPS spectra were fitted using Voigt profiles combined with their primitive functions, for inelastic backgrounds. The Gaussian width of all lines and thresholds is the same for one spectrum and does not differ considerably from one spectrum to another, being always in the range of 2 eV.

For the XPS analysis of the poisoned samples, before the analysis samples were washed with double distilled water till free of any halogen and dried under vacuum at 120 °C.

## 3. Results and discussion

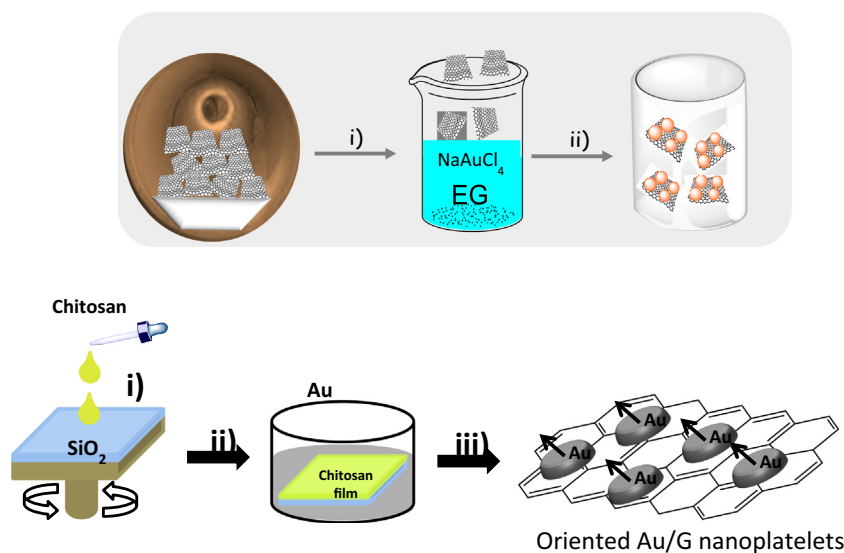
### 3.1. Catalysts preparation and characterization

In the present study, a series of Au NPs catalysts supported on few layers graphene (*fl*-G, *fl* meaning few layers, G standing for graphene) were prepared following two different procedures. In one of them, Au NPs (4–5 nm) were formed by the polyol reduction method [35] and then supported on *fl*-G present in the medium to afford Au/G as powder. In the second method, Au NPs were

formed by pyrolysis under inert atmosphere simultaneously with the formation of *fl*-G as films on quartz substrate. Scheme 1 illustrates the two different preparation methods. Attention was paid to obtain supported Au catalysts with very similar Au loading to minimize the possible influence that Au loading on G could play on the catalytic activity of the resulting materials.

In recent precedents, it has been shown that pyrolysis of chitosan films containing  $\text{HAuCl}_4$  at temperatures above 900 °C gives rise to samples in where 111 facet oriented Au nanoplatelets (20–40 lateral dimension, 3–4 nm height) are formed, becoming supported on *fl*-G films created by transformation of chitosan into G,  $\overline{\text{Au}}/\text{fl-G}$  ( $\overline{\text{Au}}$  meaning 111 oriented Au nanoplatelets) [35,36]. The insolubility of Au on carbon and the lack of formation of gold carbides determine that, during the pyrolysis, spontaneous segregation of Au as nanoplatelets occurs in the same process as the formation of G. It has been proposed that 111 facet orientation of Au derives from the “reverse template effect” of evolved G determining the preferential epitaxial growth of Au nanoplatelets with 111 facet orientation [35]. Another remarkable effect of the pyrolytic method of formation of  $\overline{\text{Au}}/\text{fl-G}$  is the strong interaction between Au nanoplatelets and *fl*-G support as reflected by: (i) the relatively small dimensions of Au platelets in spite of the high temperatures of the process (900 °C), (ii) the “wetting” of *fl*-G by Au particles having a shape as platelets rather than spherical particles observed when the Au NP-support affinity is low, and (iii) the shift about 1.4 eV toward higher values in the binding energy for Au(0) grafted on graphene as determined by XPS, meaning that there is an electron transfer from Au to graphene [35,36]. In the literature, there are evidences showing facet orientation of Au nanoplatelets based on XRD and electron microscopy and back scattered electron diffraction of  $\overline{\text{Au}}/\text{fl-G}$  [36]. Au content in  $\overline{\text{Au}}/\text{fl-G}$  was determined by ICP analysis after dissolving Au with aqua regia resulting in an amount of 3  $\text{ng}/\text{cm}^2$ .

For the sake of comparison, a sample in which randomly oriented spherical Au particles obtained by the polyol method were supported on *fl*-G was also prepared (see Scheme 1). Furthermore, analogous samples of oriented  $\overline{\text{Pd}}/\text{fl-G}$ ,  $\overline{\text{Pt}}/\text{fl-G}$  and unoriented Pd/*fl*-G and Pt/*fl*-G catalysts were prepared to compare their activity with those of Au catalysts. It was observed; however, that while  $\overline{\text{Pt}}/\text{fl-G}$  was formed similar to that of  $\overline{\text{Au}}/\text{fl-G}$  showing preferential



**Scheme 1.** Illustration of the preparation procedures leading to the formation of: Top: small Au NPs supported on G (Au/G). (i) Dispersion of G in ethylene glycol (EG), (ii) reduction of  $\text{NaAuCl}_4$  by heating at 120 °C for 24 h. Bottom: oriented 111 Au nanoplatelets on *fl*-G ( $\overline{\text{Au}}/\text{fl-G}$ ). (i) Spin coating of an aqueous solution of chitosan on clean quartz; (ii) adsorption of  $\text{Au}^{3+}$  on the chitosan film, and (iii) pyrolysis of the  $\text{Au}^{3+}$ -containing chitosan film at 900 °C under inert atmosphere.

111 facet orientation of Pt nanoplatelets, the  $\overline{Pd}/fl-G$  was not formed. Although further studies are necessary, it seems that the tendency of Pd to form carbides or the higher solubility of Pd on carbon should be responsible for the unsuccessful attempt to obtain  $\overline{Pd}/fl-G$ . Characterization data of  $\overline{Pt}/fl-G$  have been reported separately [37]. Table 1 summarizes the samples prepared, their metal content, average particle size and relevant references describing characterization data, including those related to preferential facet orientation.

### 3.2. Suzuki-Miyaura cross coupling

As commented earlier, the purpose of the present study is to determine the catalytic activity of oriented  $\overline{Au}/fl-G$  films on quartz relative to that of unoriented Au/G as suspended powder as well as respect to analogous Pd and Pt catalysts. Aimed at this objective, the coupling of phenylboronic acid with iodo-, bromo-, and chlorobenzenes in water using NaOH as base was selected as a model reaction. The observed results are summarized in Tables 2 and 3. As it can be seen in Table 2, besides biphenyl that is the expected cross coupling product, formation of ortho- and para-isomers of halobiphenyl (Scheme 2) was also observed with different selectivity.

From Table 2, it can be concluded that graphene-supported Pt catalysts, either  $\overline{Pt}/fl-G$  or Pt/G, are unable to promote the Suzuki-Miyaura coupling, regardless the halobenzene used as substrate. In contrast Au catalysts show remarkable catalytic activity, conversion and selectivity at final reaction time depending on the substrate. Unexpectedly the reactivity of chlorobenzene was much higher than that of iodobenzene.

Another important feature of Table 2 is the influence of the properties of 111 facet oriented  $\overline{Au}/fl-G$  as consequence of the preparation procedure on its catalytic activity. Comparison between the catalytic performance of  $\overline{Au}/fl-G$  and Au/G samples is somehow complicated by the fact that in the case of  $\overline{Au}/fl-G$  the catalyst is a nanometric thick film deposited on quartz with an  $1 \times 1 \text{ cm}^2$  area, while a mass of 10 mg of a powder dispersed on  $\text{H}_2\text{O}$  was used for Au/G. However, in spite that the total amount of Au present in unoriented Au/G sample was, according to chemical analysis, fifteen times higher than that of oriented  $\overline{Au}/fl-G$ , conversion for the unoriented Au/G catalysts was similar (bromobenzene) or lower (chlorobenzene) than that of the oriented sample. Specifically for the case of chlorobenzene as substrate, the turnover number (TON) under the same conditions for Au in the oriented catalyst is about 16 times higher than that of the unoriented sample. It should be noted that the particle size of Au in unoriented Au/G is about 4–6 nm which is in good accordance with the expected size of Au particles obtained by the polyol method, while those of oriented Au nanoplatelets are much larger between 20 and 40 nm. Therefore, based exclusively on Au particle size, the reverse catalytic activity, i.e.,  $\overline{Au}/fl-G$  much less active than

Au/G should have been expected. Precedents on Au catalysis have shown that the importance of the particle size on the catalytic activity that decreases dramatically as the particle size increases and typically disappears for particles larger than 10 nm [28].

It is proposed that the high activity of  $\overline{Au}/fl-G$  arises from the strong Au nanoplatelet-graphene interaction. In catalysis by supported Au NPs, it is a general observation that the nature of the support plays a notable role on the catalytic activity of the sample [39–41]. The shift in the XPS binding energy of Au nanoplatelets indicates that these particles should bear a partial positive charge density as compared to bulk Au metal and this charge transfer from Au to graphene not observed on Au/G could be one of the reasons for their high catalytic activity. In addition, other factor that should be playing a role is the crystallographic orientation of Au nanoplatelets in the 111 facet and the possible steps on the platelets. Whatever the origin of this remarkable catalytic activity for  $\overline{Au}/fl-G$ , it agrees with earlier observations on a remarkably high activity of metal NPs (Au, Pt and Cu) grafted on G prepared by pyrolysis for homocouplings, oxidations and as photocatalysts [35–37,42].

#### 3.2.1. Au versus Pd catalysts

As expected, Pd/G also exhibits a notable catalytic activity to promote Suzuki-Miyaura cross coupling. A detailed comparison between the two metals is provided in Table 3 that shows activity data for the three halobenzenes at different reaction temperatures in the range of 70–100 °C.

As it can be seen there, except for those reactions carried out at 70 °C, the activity of  $\overline{Au}/fl-G$  was always similar, but somewhat lower, than that of Pd/G under the conditions indicated in Table 3. As commented above, when comparing the data between  $\overline{Au}/fl-G$  and Pd/G, the possible differences in the experimental conditions between films deposited on quartz ( $\overline{Au}/fl-G$ ) and dispersed powders (Pd/G) and the metal loadings have to be noticed. In any case, data from Table 3 consistently shows that, when TONs at 4 h reaction and turnover frequencies (TOFs) based on initial reaction rates are considered, the catalytic activity of  $\overline{Au}/fl-G$  is always three orders of magnitude higher than that of the Pd/G. Since the average particle size of Pd NPs in Pd/G is 3–4 nm, while that of  $\overline{Au}/fl-G$  is (3–4 × 20–40 nm), the substantially higher catalytic activity of  $\overline{Au}/fl-G$  is again remarkable.

Another general conclusion from Table 3 is that the activation energy for  $\overline{Au}/fl-G$  and Pd/G follows the same trends and is higher by a factor about 3 for chlorobenzene than for iodobenzene for both metals. This trend agrees with the relative order of C–X bond energies and is in accordance with the relative reactivity order observed for Pd catalysts. However, it contrasts with the results obtained at long reaction times, previously commented in Table 2 (entries 2, 6 and 13), wherein chlorobenzene reached higher conversion than bromobenzene and this is higher than iodobenzene.

**Table 1**  
Details of various catalysts used in the present study.

Catalyst	Metal content	Particle size(nm)	Preparation method	Refs. <sup>a</sup>
Au/G	0.01 wt%	4–6	Polyol	[35]
Pd/G	1 wt%	3–4	Polyol	[38]
Pt/G	1 wt%	2	Polyol	[37]
$\overline{Au}/fl-G$	3 ng/cm <sup>2</sup>	20–40	Pyrolysis	[35]
$\overline{Pd}/fl-G$	Unsuccessful preparation			
$\overline{Pt}/fl-G$	5 ng/cm <sup>2</sup>	20–40	Pyrolysis	[37]

<sup>a</sup> For complete characterization data refer to the original publication of the preparation of these materials.

**Table 2**  
Catalytic activities of oriented and unoriented Au and Pt on graphene in Suzuki-Miyaura coupling reactions.<sup>a</sup>

Run	Aryl halide	Catalyst	Conversion (%) <sup>b</sup>	S <sub>B</sub> (%) <sup>b</sup>	S <sub>oB</sub> (%) <sup>b</sup>	S <sub>pB</sub> (%) <sup>b</sup>
1	Ph-I	Au/G	51.3	81.4	5.8	12.8
2		$\overline{Au}/fl-G$	2.4	85.5	3.1	11.4
3		$\overline{Pt}/fl-G$	1.5	86.5	3.1	10.4
4		Pt/G	0.9	62.9	33.5	3.6
5	Ph-Br	Au/G	>99.9	36.0	50.7	13.3
6		$\overline{Au}/fl-G$	90.9	39.9	49.2	10.9
7		$\overline{Pt}/fl-G$	0.9	50.3	31.2	17.8
8		Pt/G	0.2	77.8	11.0	11.2
9		$\overline{Au}/fl-G^c$	71.4	23.6	39.5	36.9
10		$\overline{Au}/fl-G^d$	82.3	63.0	19.2	17.8
11		$\overline{Au}/fl-G^e$	87.8	60.8	26.1	13.1
12	Ph-Cl	Au/G	81.7	58.6	26.5	14.9
13		$\overline{Au}/fl-G$	100	65.0	24.9	10.1
14		$\overline{Pt}/fl-G$	0.2	51.0	42.7	6.3
15		Pt/G	0	0	0	0

<sup>a</sup> Reaction conditions: halobenzene (2 mmol), phenylboronic acid (2.4 mmol), deionized water (20 mL), NaOH (8 mmol), 80 °C, under reflux, 24 h. Catalyst: 10 mg for Au/G or Pt/G and 1 × 1 cm<sup>2</sup> films deposited on quartz in the cases of  $\overline{Au}/fl-G$  and  $\overline{Pt}/fl-G$  samples.

<sup>b</sup> Determined by GC-MS.

<sup>c</sup> With 0.2 mmol of KI.

<sup>d</sup> With 0.2 mmol of KBr.

<sup>e</sup> With 0.2 mmol of KCl.

**Table 3**  
Results of the Suzuki-Miyaura coupling catalyzed by  $\overline{Au}/fl-G$  or Pd/G for halobenzenes at four different temperatures.<sup>a</sup>

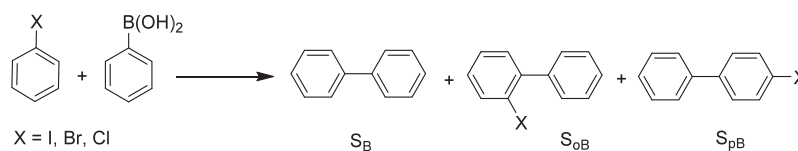
Run	Catalyst	T(°C)	Conversion (%)	TON <sup>b</sup>	TOF (s <sup>-1</sup> ) <sup>c</sup>	Activation energy (kJ/mol) <sup>d</sup>
I	$\overline{Au}/fl-G$	70	44.5	0.19 × 10 <sup>8</sup>	13.3 × 10 <sup>2</sup>	26
		80	58.5	0.25 × 10 <sup>8</sup>	17.2 × 10 <sup>2</sup>	
		90	72.5	0.31 × 10 <sup>8</sup>	21.6 × 10 <sup>2</sup>	
		100	92.0	0.39 × 10 <sup>8</sup>	27.3 × 10 <sup>2</sup>	
	Pd/G	70	27.5	0.058 × 10 <sup>5</sup>	0.40	20
		80	70.5	0.151 × 10 <sup>5</sup>	1.05	
		90	86.0	0.183 × 10 <sup>5</sup>	1.27	
		100	99.9	0.212 × 10 <sup>5</sup>	1.48	
Br	$\overline{Au}/fl-G$	70	16.0	0.07 × 10 <sup>8</sup>	4.97 × 10 <sup>2</sup>	41
		80	23.5	0.10 × 10 <sup>8</sup>	7.13 × 10 <sup>2</sup>	
		90	37.0	0.16 × 10 <sup>8</sup>	11.19 × 10 <sup>2</sup>	
		100	50.3	0.22 × 10 <sup>8</sup>	15.70 × 10 <sup>2</sup>	
	Pd/G	70	27.0	0.057 × 10 <sup>5</sup>	0.39	44
		80	37.0	0.079 × 10 <sup>5</sup>	0.55	
		90	62.0	0.132 × 10 <sup>5</sup>	0.92	
		100	89.8	0.189 × 10 <sup>5</sup>	1.31	
Cl	$\overline{Au}/fl-G$	70	3.5	0.015 × 10 <sup>8</sup>	1.06 × 10 <sup>2</sup>	59
		80	7.0	0.031 × 10 <sup>8</sup>	2.15 × 10 <sup>2</sup>	
		90	11.0	0.048 × 10 <sup>8</sup>	3.37 × 10 <sup>2</sup>	
		100	18.5	0.015 × 10 <sup>8</sup>	5.50 × 10 <sup>2</sup>	
	Pd/G	70	4.4	0.009 × 10 <sup>5</sup>	0.06	66
		80	8.0	0.017 × 10 <sup>5</sup>	0.12	
		90	14.0	0.030 × 10 <sup>5</sup>	0.21	
		100	26.0	0.055 × 10 <sup>5</sup>	0.38	

<sup>a</sup> Reaction conditions: PhX 2.00 mmol, PhB(OH)<sub>2</sub> 2.4 mmol, deionized H<sub>2</sub>O 20 mL, NaOH 8 mmol, reaction time 4 h, temperature as indicated. Catalyst:  $\overline{Au}/fl-G$  films 1 × 1 cm<sup>2</sup> and Pd/G powder 10 mg.

<sup>b</sup> Calculated by dividing the moles of substrate converted at 4 h by the moles of metal present in the catalyst.

<sup>c</sup> Calculated dividing TON by time.

<sup>d</sup> Calculated from the Arrhenius plot.



**Scheme 2.** Suzuki-Miyaura coupling reaction with oriented and unoriented Au and Pt based catalysts.

### 3.3. Poisoning experiments

In order to understand the reverse reactivity order of halobenzenes in the present  $\overline{\text{Au}}/\text{fl-G}$  catalytic system, a series of control experiments in the presence of KX (10% with respect to the amount of PhBr) were conducted using bromobenzene as substrate. Note that since the reactions are carried out in water, all these salts were totally soluble. Bromobenzene was selected for this poisoning study, since it allows to observe an increase or decrease in the catalytic activity in the presence of the added KX salt. Thus, when the

reaction of phenylboronic acid and bromobenzene using  $\overline{\text{Au}}/\text{fl-G}$  as catalyst was performed in the presence of KX at initial time, a decrease in conversion from 90.9% to 71.4% and 82.3% (entries 9–10, Table 2) was observed when the reaction is carried in the presence of KI and KBr, respectively, while the presence of KCl as additive has a negligible influence (87.8%, entry 11, Table 2). These activity data is compatible with a poisoning effect of KX salts, particularly for  $\text{I}^-$ .

To confirm this poisoning effect for  $\text{I}^-$  and in lower extent  $\text{Br}^-$ , providing some insight into the reasons for the much higher

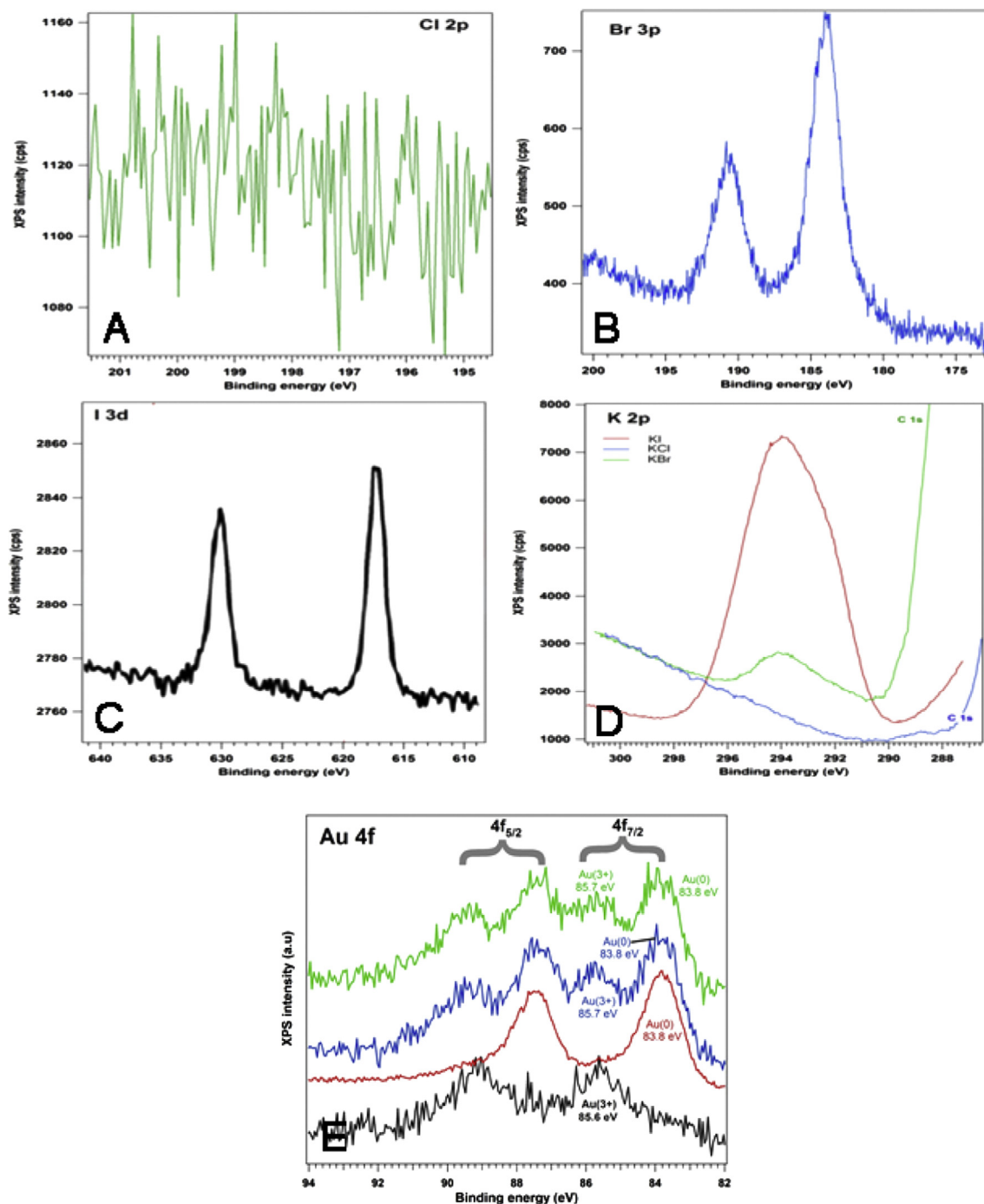


**Fig. 1.** XPS spectra collected in the region of the  $\text{Cl}_{2p}$ ,  $\text{Br}_{3p}$ ,  $\text{I}_{3d}$ ,  $\text{K}_{2p}$  and  $\text{Au}_{4f}$  binding energy values for the recovered  $\overline{\text{Au}}/\text{fl-G}$  films in the Suzuki-Miyaura reaction of halobenzenes in the presence of the three KX salts. Reaction conditions: halobenzene (2 mmol), phenylboronic acid (2.4 mmol), deionized water (20 mL), NaOH (8 mmol), KX (X: Cl, Br and I, 0.2 mmol), temperature 80 °C, under reflux, 24 h. Red: fresh  $\overline{\text{Au}}/\text{fl-G}$  catalyst, blue: after the reaction of chlorobenzene, green: after the reaction of bromobenzene, and black: after the reaction of iodobenzene.

activity of Au catalysts for chlorobenzene than for iodobenzene, the oriented  $\overline{\text{Au}}/\text{fl-G}$  samples recovered after the reactions were characterized by XPS, trying to monitor the presence of halides. As expected, after the reaction with iodo- and bromobenzene, XPS detected the presence of both elements iodo and bromo on the films. In contrast, similar measurement for chlorobenzene failed to detect the presence of chlorine on the  $\overline{\text{Au}}/\text{fl-G}$ , in spite that the conversion of chlorobenzene was complete and much larger concentrations of  $\text{Cl}^-$  than  $\text{I}^-$  should be present in  $\text{H}_2\text{O}$ . These data indicate that under the reaction conditions Au nanoplatelets adsorb large amounts of iodo and bromo, but not chloro. It is interesting to remark that the presence of iodo detected on the  $\overline{\text{Au}}/\text{fl-G}$  after its use as catalyst gives a significant atomic percentage in spite of the low conversion in which the reaction took place (entry 2, Table 2). These results suggest that iodide and bromide could act as a poison of Au by interacting strongly with the surface of these metal particles. In contrast, the interaction with chloride should be much lower and apparently no poisoning is taking place. These results agree with the ones previously reported for Au NPs supported on  $\text{CeO}_2$  [43] wherein a strong adsorption of  $\text{I}^-$  on the Au/ $\text{CeO}_2$  catalyst was responsible for a decrease in activity during the Sonogashira coupling between phenylacetylene and iodobenzene.

Similar XPS analysis was also performed for the  $\overline{\text{Au}}/\text{fl-G}$  films used in the previously commented KX poisoning tests. After the reaction we were able to detect also  $\text{K}^+$  when KI or KBr was added as poisons, while no  $\text{K}^+$  was detected for KCl as poison. Fig. 1 summarizes these results. Thus, these XPS analyses indicate that the presence of chloride is never detected adsorbed in the  $\overline{\text{Au}}/\text{fl-G}$  film either when chlorobenzene is the substrate or when bromobenzene is used as substrate and KCl as poison. In contrast, in the case of iodide a considerable proportion of KI is present on the film and both  $\text{I}^-$  and  $\text{K}^+$  are detected. Thus, all the available catalytic data indicate that the activity of Au nanoplatelets for the Suzuki coupling is also controlled by the strength of the C–X bond as in the case of Pd catalysis [44], but as the reaction progresses by the strong adsorption of  $\text{I}^-$  on Au atoms at the surface of the particles causes their deactivation, a fact that is not observed for Pd catalysts.

Besides the presence of halides, Fig. 1e also shows the XPS spectra of the  $\text{Au}_{4f}$  level for the fresh and catalysts tested with the different halobenzenes. Fresh catalyst (red) exhibited only bands assigned to Au(0) nanoparticles. Spectra collected for the catalysts reacted with chloro- and bromobenzene still preserve the binding energies of the bands of the Au(0) species (bands located at 83.8 eV) [45]. However, new bands located at binding energies of 85.7 eV and assigned to Au(III) species [46] have also been evidenced. Very differently to these spectra, working with iodobenzene produced a complete oxidation of Au (0) to Au(III) species. This is in agreement with the high concentration of  $\text{I}^-$  observed in this sample as commented earlier. However, the oxidized species do not leach out from graphene to the solution as ICP-OES analysis of the hot liquid phase and recycling did not show any other change in the XPS spectra.

The presence of the Au(0)/Au(III) couple may recall the results of the reported efforts to combine gold and palladium catalysis for C–C coupling reactions where the positive effect was attributed to a transmetalation from gold compounds to palladium [47–49]. The two species may concert in a similar manner.

### 3.4. Agreement with theoretical calculations

Previously reported theoretical calculations on the adsorption of halobenzenes on Au clusters provide deeper insight into the origin of the relative halobenzene activity order of Au catalysts [43].

Thus, adsorption of iodobenzene on  $\text{Au}_{53}$  clusters has shown that the C–I bond should be broken in the process, the adsorbate having new Au–Ph and Au–I bonds [43]. Similarly, these calculations have shown that bromobenzene adsorbs weaker than iodobenzene on  $\text{Au}_{53}$  clusters, but it also forms Au–Ph and Au–Br bonds. In contrast, these DFT calculations have indicated that the strength of the C–Cl bond determines that no chemisorption should occur on  $\text{Au}_{53}$  and only a small elongation of the C–Cl bond should be expected on the adsorption. Accordingly, these theoretical calculations predict the strong binding of Au to iodo, but not chlorine, in the adsorption of the aryl halides.

It is proposed that this strong binding between Au and iodide will cause catalyst deactivation, while no similar deactivation would occur in the case of aryl chloride. It has to be also commented that these calculations indicate that the activation energy for aryl chloride on Au is higher than for Ph–I that has lower activation energy, as it has been experimentally observed here [43]. Therefore, poisoning iodide as leaving group is the most likely reason for the apparent low activity of Au particles in the Suzuki–Miyaura coupling.

## 4. Conclusions

The present manuscript has shown that Au particles supported on G are able to promote Suzuki–Miyaura coupling wherein chlorobenzene exhibits much higher reactivity than iodobenzene. This low relative reactivity of iodoarenes arises from the strong Au deactivation caused by iodide adsorption on Au particles, resulting in the experimental detection of iodo on  $\overline{\text{Au}}/\text{fl-G}$  film after the reaction. Also, it has been found that strong grafting of Au on G and preferential 111 facet orientation increase the activity respect to analogous samples of randomly oriented Pd NPs supported on G by three orders of magnitude. This higher catalytic activity of  $\overline{\text{Au}}/\text{fl-G}$  films is even more remarkable considering that it is against the general relationship between small particle size and activity. The high activity of  $\overline{\text{Au}}/\text{fl-G}$  can serve to develop more efficient coupling catalysts, having implication in organic synthesis.

## Acknowledgments

ADM thanks University Grants Commission (UGC), New Delhi for the award of Assistant Professorship under its Faculty Recharge Programme. ADM also thanks Department of Science and Technology, India, for the financial support through Extra Mural Research funding (SB/FT/CS-166/2013) and the Generalidad Valenciana for financial aid supporting his stay at Valencia through the Prometeo programme. Financial support by the Spanish Ministry of Economy and Competitiveness (CTQ-2012-32315 and Severo Ochoa) and Generalidad Valenciana (Prometeo 2012-014) is gratefully acknowledged. The research leading to these results has received partial funding from the European Community's Seventh Framework Programme (FP7/2007–2013) under grant agreement no. 228862.

## References

- [1] N. Miyaura, A. Suzuki, *Chem. Commun.* (1979) 866.
- [2] R. Martin, S.L. Buchwald, *Acc. Chem. Res.* 41 (2008) 1461.
- [3] N. Miyaura, A. Suzuki, *Chem. Rev.* 95 (1995) 2457.
- [4] C.C.C. Johansson Seechurn, M.O. Kitching, T.J. Colacot, V. Snieckus, *Angew. Chem. Int. Ed.* 51 (2012) 5062.
- [5] A. Balog, D. Meng, T. Kamenecka, P. Bertinato, D.-S. Su, E.J. Sorensen, S.J. Danishefsky, *Angew. Chem. Int. Ed.* 35 (1996) 2801.
- [6] J. Liu, S.D. Lotesta, E.J. Sorensen, *Chem. Commun.* 47 (2011) 1500.
- [7] J.R. Vyvyan, E.A. Peterson, M.L. Stephan, *Tetrahedron Lett.* 40 (1999) 4947.
- [8] T.E. Jacks, D.T. Belmont, C.A. Briggs, N.M. Horne, G.D. Kanter, G.L. Karrick, J.J. Krikke, R.J.N. McCabe, J.G. Mustakis, T.N. Nanninga, G.S. Risedorph, R.E.

- Seamans, R. Skeeane, D.D. Winkle, T.M. Zennie, *Org. Proc. Res. Develop.* 8 (2004) 201.
- [9] A.L. Casalnuovo, J.C. Calabrese, *J. Am. Chem. Soc.* 112 (1990) 4324.
- [10] F.-S. Han, *Chem. Soc. Rev.* 42 (2013) 5270.
- [11] A. Dhakshinamoorthy, A.M. Asiri, H. Garcia, *Chem. Soc. Rev.* 44 (2015) 1922.
- [12] I. Kondolff, H. Doucet, M. Santelli, *Tetrahedron* 60 (2004) 3813.
- [13] Y. Chen, H. Peng, Y.-X. Pi, T. Meng, Z.-Y. Lian, M.-Q. Yan, Y. Liu, S.-H. Liu, G.-A. Yu, *Org. Biomol. Chem.* 13 (2015) 3236.
- [14] J.H. Kirchhoff, M.R. Netherton, I.D. Hills, G.C. Fu, *J. Am. Chem. Soc.* 124 (2002) 13662.
- [15] H. Doucet, *Eur. J. Org. Chem.* (2008) 2013.
- [16] S.K. Hashmi, C. Lothschütz, C. Böhlring, F. Rominger, *Organometallics* 30 (2011) 2411.
- [17] A. Roucoux, J. Schulz, H. Patin, *Chem. Rev.* 102 (2002) 3757.
- [18] C. Xu, X. Wang, J. Zhu, *J. Phys. Chem. C* 112 (2008) 19841.
- [19] D. Astruc, F. Lu, J.R. Aranzas, *Angew. Chem. Int. Ed.* 44 (2005) 7852.
- [20] N.T.S. Phan, M. Van Der Sluys, C.W. Jones, *Adv. Synth. Catal.* 348 (2006) 609.
- [21] L. Yin, J. Liebscher, *Chem. Rev.* 107 (2007) 133.
- [22] S. Hübner, J.G. de Vries, V. Farina, *Adv. Synth. Catal.* 358 (2016) 3.
- [23] D. Astruc, *Nanoparticles and Catalysis*, Wiley-VCH, Weinheim, 2008.
- [24] M.M. Manas, R. Pleixats, *Acc. Chem. Res.* 36 (2003) 638.
- [25] K. Sawai, R. Tatum, T. Nakahodo, H. Fujihara, *Angew. Chem. Int. Ed.* 47 (2008) 6917.
- [26] D. Zim, V.R. Lando, J. Dupont, A.L. Monteiro, *Org. Lett.* 3 (2001) 3049.
- [27] M.B. Thathagar, J. Beckers, G. Rothenberg, *J. Am. Chem. Soc.* 124 (2002) 11858.
- [28] J. Han, Y. Liu, R. Guo, *J. Am. Chem. Soc.* 131 (2009) 2060.
- [29] D.K. Dumbre, P.N. Yadav, S.K. Bhargava, V.R. Choudhary, *J. Catal.* 301 (2013) 134.
- [30] N. Zhang, H. Qiu, Y. Liu, W. Wang, Y. Li, X. Wang, J. Gao, *J. Mater. Chem.* 21 (2011) 11080.
- [31] A. Corma, R. Juárez, M. Boronat, F. Sanchez, M. Iglesias, H. Garcia, *Chem. Commun.* 47 (2011) 1446.
- [32] C. Gonzalez-Arellano, A. Abad, A. Corma, H. Garcia, M. Iglesias, F. Sanchez, *Angew. Chem. Int. Ed.* 46 (2007) 1536.
- [33] S. Witzel, J. Xie, M. Rudolph, A.S.K. Hashmi, *Adv. Synth. Catal.* 359 (2017), <http://dx.doi.org/10.1002/adsc.201700121>.
- [34] A.M. Echavarren, A.S.K. Hashmi, F.D. Toste, *Adv. Synth. Catal.* 358 (2016) 1347.
- [35] A. Primo, I. Esteve-Adell, S.N. Coman, N. Candu, V.I. Parvulescu, H. Garcia, *Angew. Chem. Int. Ed.* 55 (2016) 607.
- [36] D. Mateo, I. Esteve-Adell, J. Albero, J.F. Sanchez Royo, A. Primo, H. Garcia, *Nat. Commun.* 7 (2016) 11819.
- [37] I. Esteve-Adell, N. Bakker, A. Primo, E. Hensen, H. García, *ACS Appl. Mater. Interf.* 8 (2016) 33690.
- [38] J.F. Blandez, I. Esteve-Adell, M. Alvaro, H. Garcia, *Catal. Sci. Technol.* 5 (2015) 2167.
- [39] M. Haruta, *Catal. Today* 36 (1997) 153.
- [40] M. Haruta, *Cattech* 6 (2002) 102.
- [41] M. Haruta, S. Tsubota, T. Kobayashi, H. Kageyama, M.J. Genet, B. Delmon, *J. Catal.* 144 (1993) 175.
- [42] D. Mateo, I. Esteve-Adell, J. Albero, A. Primo, H. García, *Appl. Catal., B* 201 (2017) 582.
- [43] M. Boronat, D. Combita, P. Concepción, A. Corma, H. García, R. Juárez, S. Laursen, J. de Dios López-Castro, *J. Phys. Chem. C* 116 (2012) 24855.
- [44] G.C. Fu, *Acc. Chem. Res.* 41 (2008) 1555.
- [45] N.H. Turner, A.M. Single, *Surf. Interf. Anal.* 15 (1990) 215.
- [46] W.A. Pireaux, M. Leibr, P.A. Thiry, J.P. Delrue, R. Caudano, *Surf. Sci.* 141 (1984) 221.
- [47] A.S.K. Hashmi, C. Lothschütz, R. Döpp, M. Ackermann, J. De Buck Becker, M. Rudolph, C. Scholz, F. Rominger, *Adv. Synth. Catal.* 354 (2012) 133.
- [48] A.S.K. Hashmi, R. Döpp, C. Lothschütz, M. Rudolph, D. Riedel, F. Rominger, *Adv. Synth. Catal.* 352 (2010) 1307.
- [49] A.S.K. Hashmi, C. Lothschütz, R. Dopp, M. Rudolph, T.D. Ramamurthi, F. Rominger, *Angew. Chem. Int. Ed.* 48 (2009) 8243.